Available online at www.sciencedirect.com
ScienceDirect
Catalysis Today 117 (2006) 447–453
CATALYSIS TODAY
www.elsevier.com/locate/cattod

Fuel-rich catalytic combustion of methane in zero emissions power generation processes

S. Eriksson [a,*], M. Wolf [b], A. Schneider [c], J. Mantzaras [c], F. Raimondi [c], M. Boutonnet [a], S. Järås [a]

[a] *Royal Institute of Technology, Chemical Technology, Teknikringen 42, SE-100 44 Stockholm, Sweden*
[b] *ALSTOM Power, Technology Center, Segelhof, CH-5405 Baden-Dättwil, Switzerland*
[c] *Paul Scherrer Institut, CH-5232 Villigen PSI, Switzerland*

Available online 17 July 2006

Abstract

A novel catalytic combustion concept for zero emissions power generation has been investigated. Catalysts consisting of Rh supported on ZrO_2, Ce-ZrO_2 or α-Al_2O_3 were prepared and tested under fuel-rich conditions, i.e. for catalytic partial oxidation (CPO) of methane. The experiments were performed in a subscale gas-turbine reactor operating at 5 bar with exhaust gas-diluted feed mixtures.

The catalyst support material was found to influence the light-off temperature significantly, which increased in the following order Rh/Ce-ZrO_2 < Rh/ZrO_2 < Rh/α-Al_2O_3. The Rh loading, however, only had a minor influence. The high activity of Rh/Ce-ZrO_2 is probably related to the high dispersion of Rh on Ce-ZrO_2 and the high oxygen mobility of this support compared to pure ZrO_2. The formation of hydrogen was also found to increase over the catalyst containing ceria in the support material.

Keywords: Catalytic combustion; Catalytic partial oxidation (CPO) of methane; AZEP; Rhodium catalysts; Ceria

1. Introduction

An increasing concern regarding environmental pollution during the last years has resulted in stricter emission regulations for NO_x, SO_x and greenhouse gases. Due to these, and potentially more demanding future restrictions, there is a need to improve existing power generation processes. The advanced zero emission power (AZEP) concept enables NO_x elimination as well as cost reduction of CO_2 separation compared to conventional techniques (tail-end-capture) [1]. These targets can be achieved by (i) combusting natural gas in pure oxygen produced by a mixed conductive membrane (MCM) in which O_2 is separated from air and (ii) dilution of the fuel/oxygen mixture with combustion products, i.e. water and carbon dioxide. The AZEP concept is described in Fig. 1.

The high amounts of steam and carbon dioxide present in the AZEP process, i.e. about 50 and 25%, respectively, render homogeneous ignition of the fuel mixture particularly challenging. On the other hand, catalytic combustion is an attractive alternative. The commonly used catalysts for methane combustion in lean air mixtures are based on palladium. However, several studies have shown that water severely inhibits the activity of palladium [2–4], while other materials like rhodium could be less sensitive. Therefore, a two-stage process has been investigated, wherein catalytic partial oxidation (CPO) of fuel-rich methane/oxygen mixtures over Rh is used to stabilize a subsequent overall fuel-lean homogeneous combustion zone. Syngas, H_2 and CO, is catalytically produced under fuel-rich conditions resulting in hydrogen stabilized flame combustion. The advantages of the fuel-rich approach in terms of light-off and hydrogen selectivity have been reported earlier [5] for CH_4/air mixtures without exhaust gas dilution in the same subscale gas-turbine reactor as the one used in the present investigation. For the catalytic systems used in the fuel-rich first stage of the AZEP process, low light-off temperatures and high syngas selectivities are required. Rh-based catalysts have shown the required properties yet in great variation with respect to support materials, noble metal loading, etc. [6].

In this study, catalysts for the first fuel-rich step of this process were investigated. Various supported rhodium catalysts

* Corresponding author. Tel.: +46 87909150; fax: +46 8108579.
E-mail address: sarae@ket.kth.se (S. Eriksson).

0920-5861/$ – see front matter © 2006 Elsevier B.V. All rights reserved.
doi:10.1016/j.cattod.2006.06.010

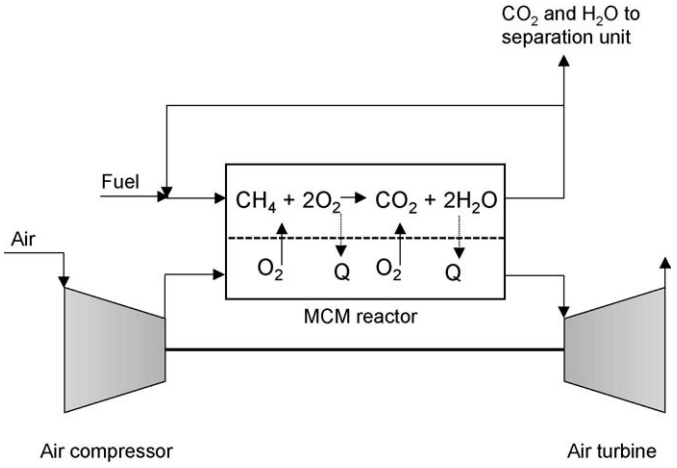

Fig. 1. Description of the AZEP concept with the MCM reactor unit.

have been prepared and tested in a high-pressure subscale gas-turbine test rig under AZEP conditions. The influence of support material, oxygen-to-fuel ratio and Rh loading on the methane conversion and outlet gas composition was studied.

2. Experimental

Supported rhodium catalysts were prepared by the incipient wetness impregnation technique using $Rh(NO_3)_3$ as metal precursor. The support materials had previously been calcined at 1073 K for 5 h. The only exception was alumina, which was calcined at 1373 K for 10 h to obtain the α-Al_2O_3 phase. The impregnated powders (0.5–2 wt% noble metal loading) were dried at 383 K and calcined at 873 K for 5 h before coating on FeCrAlloy metal. The coated FeCrAlloy was assembled to a fully coated honeycomb structure with a diameter of 35 mm a total length of 75 mm, and a coated central length of 50 mm. Each honeycomb structure contained about 7 g of catalyst material.

The experiments were carried out in a high-pressure subscale gas-turbine test rig, which has been described in more detail elsewhere [5]. Sheathed thermocouples monitored the temperature at the reactor entry and exit and at different axial locations of dedicated catalytic channels. The catalyst was not externally heated or cooled and, thus, the reactor operated under near adiabatic conditions. All reactants and products except H_2O were analyzed by gas chromatography. The water concentration was calculated using element balances. A gas mixture consisting of 83–132 nl/min CH_4, 67 nl/min O_2, 150 nl/min CO_2 and 300 nl/min H_2O was fed to the reactor, which operated at a pressure of 5 bar and a gas hourly space velocity (GHSV) of $8 \times 10^5\ h^{-1}$. The flow rate of CH_4 was varied in order to obtain different oxygen-to-fuel ratios, i.e. $\lambda = 0.25$–0.4.

The BET surface area of the catalyst powders was measured by N_2 adsorption using a Micromeritics ASAP 2010 instrument. The samples were degassed at 523 K prior to analysis. Temperature programmed reduction (TPR) experiments were performed on a Micromeritics AutoChem 2910 instrument. The samples (0.25 g) were pretreated in Ar at 473 K for 30 min before reduction. The reduction was carried out in 5% H_2/Ar (30 ml/min) by heating the sample from room temperature to 1073 K at a heating rate of 10 K/min. The noble metal dispersion was determined by H_2 chemisorption analysis performed on a Quantachrome Autosorb-1C instrument. The samples were reduced in H_2 (50 ml/min) at 673 K for 1 h followed by evacuation (673 K for 1 h) prior to the analysis. The adsorption measurements were performed at 195 K using H_2 as adsorptive and assuming a H_2:Rh = 1:2 stoichiometry. The adsorption temperature of 195 K was used in order to suppress spill-over of hydrogen to the support, which has been reported to occur for ceria-containing support materials under certain conditions [7]. The metal dispersion was calculated according to the dual isotherm method.

Catalyst-coated FeCrAlloy samples were analyzed by X-ray photoelectron spectroscopy (XPS) and Raman microscopy. Selected samples were analyzed both before and after the activity tests to determine any structural changes occurring under reaction conditions. XPS experiments were performed in a VG Escalab 220i XL apparatus, using Mg Kα radiation. The electron analyser was used in the constant pass energy mode with a pass energy of 20 eV. The pressure in the analysis chamber during the measurements was always better than 10^{-9} mbar. The composition of the surface and sub-surface regions accessible by XPS was calculated from the intensity of the XPS peaks using the transmission function of the electron analyser and the photoemission cross-sections calculated by Scofield [8]. Charging during the XPS experiments was in all cases smaller than 10 eV. Charge correction was carried out setting the C 1s peak of adventitious carbon to a value of 285.0 eV. After charge correction, the Zr $3d_{5/2}$ peak was always centred at 182.3 ± 0.2 eV, consistent with the presence of Zr(IV) [9]. This supports the validity of the applied charge correction method.

The catalyst samples were studied with a confocal Raman microscope (Labram, DILOR) equipped with a 100× magnification objective (laser spot size $0 \leq 1$ μm) and a thermoelectrically cooled charge coupled device (CCD) detector (1152×300 pixels). The Raman spectra were obtained in a backscattering geometry with the 632.8 nm line of a He–Ne laser. The power at the sample was ~4 mW. Raman spectra were routinely recorded in the range from 100 to 1100 cm^{-1} using a 1800 grooves/mm grating. The lateral resolution of the Raman microscope was about 2 μm.

3. Results

3.1. Catalyst characterization

The characteristics of the Rh catalysts are presented in Table 1. The BET surface area for the Rh/ZrO_2 catalysts was about 20 m^2/g whereas a higher value of 44 m^2/g could be measured for Rh/Ce-ZrO_2. The lowest surface area was detected for Rh/α-Al_2O_3 (6 m^2/g). The metal dispersion values calculated from H_2 chemisorption experiments varied in the range 17–54%. The temperature programmed reduction

Table 1
Catalyst characteristics

Catalyst	BET surface area [m^2/g]	Metal dispersion [%]	T_{red}[a] [K]
0.5% Rh/ZrO_2	22	21	343, 377
1% Rh/ZrO_2	21	20	353, 379
2% Rh/ZrO_2	17	17	352, 378
1% Rh/α-Al_2O_3	6	20	392
1% Rh/Ce-ZrO_2	44	54	338

[a] Temperature for Rh reduction peak(s). The maximum value of the reduction peak is reported.

experiments show that rhodium oxide (Rh_2O_3) is completely reduced at $T < 473$ K for all catalysts. The lowest reduction temperature was obtained for 1% Rh/Ce-ZrO_2. For the ZrO_2 supported catalysts two peaks could be identified. The existence of two reduction peaks may be attributed to a nonuniform size distribution of rhodium particles. The peak at a lower reduction temperature was always considerably smaller than the other one.

The Rh 3d photoelectron spectra and Raman microscopy results of selected catalyst samples are presented in Fig. 2. In Fig. 2a, the spectra for fresh and used Rh/ZrO_2 are shown. The peak maximum of the Rh $3d_{5/2}$ transition was located at 308.8 eV in the fresh sample, which corresponds to Rh_2O_3 [10,11]. In the used sample, the intensity of the Rh^{3+} peak has decreased significantly and a shift in peak maximum to 308.0 eV can be observed. This observation is in agreement with a partial reduction of Rh^{3+} to metallic rhodium. The metallic Rh state is characterized by a lower binding energy of 307–307.4 eV [10,11] for the Rh $3d_{5/2}$ photoelectron peak compared to Rh^{3+} (308.2–309.4 eV). The results show that the reaction conditions affect the state of surface Rh species resulting in a partial reduction of Rh^{3+} to Rh^0.

In Fig. 2b, Rh 3d spectra for used catalysts consisting of different support materials are presented. Here, the degree of reduction of Rh^{3+} to Rh^0 can be estimated by comparing the relative intensities of the corresponding peaks as indicated by dashed lines. The results show that the fraction of metallic rhodium after the CPO reaction is higher for 2% Rh/ZrO_2 than 1% Rh/Ce-ZrO_2.

Crystal phases of the support materials for fresh and used catalysts could be determined by Raman microscopy as shown in Fig. 2c and d. The different crystal phases, i.e. tetragonal and monoclinic ZrO_2, are indicated by dashed lines. Both the monoclinic and tetragonal phase of ZrO_2 is present for the fresh 1% Rh/ZrO_2 catalyst whereas only the monoclinic phase could be detected after testing. However, when Ce is incorporated in the zirconia structure, only the tetragonal phase was identified for the fresh as well as the used catalyst. The catalyst temperature exceeded 1073 K, which is the calcination temperature for the support, for short periods during all tests performed at $\lambda = 0.4$. This explains the phase transition of ZrO_2 to pure monoclinic phase. The tetragonal ZrO_2 phase is stable at

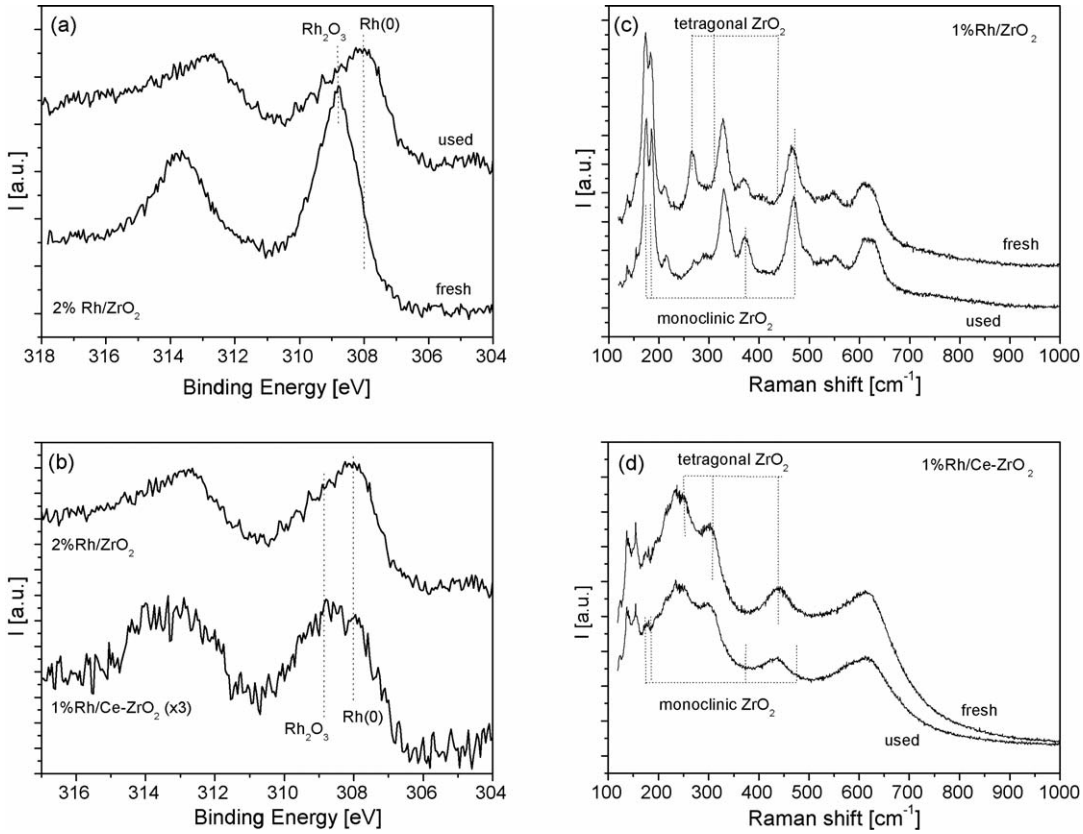

Fig. 2. Rh 3d XPS peaks for (a) fresh and used 2% Rh/ZrO_2, and (b) used 2% Rh/ZrO_2 and 1% Rh/Ce-ZrO_2. Raman spectra of fresh and used (c) 1% Rh/ZrO_2 and (d) 1% Rh/Ce-ZrO_2.

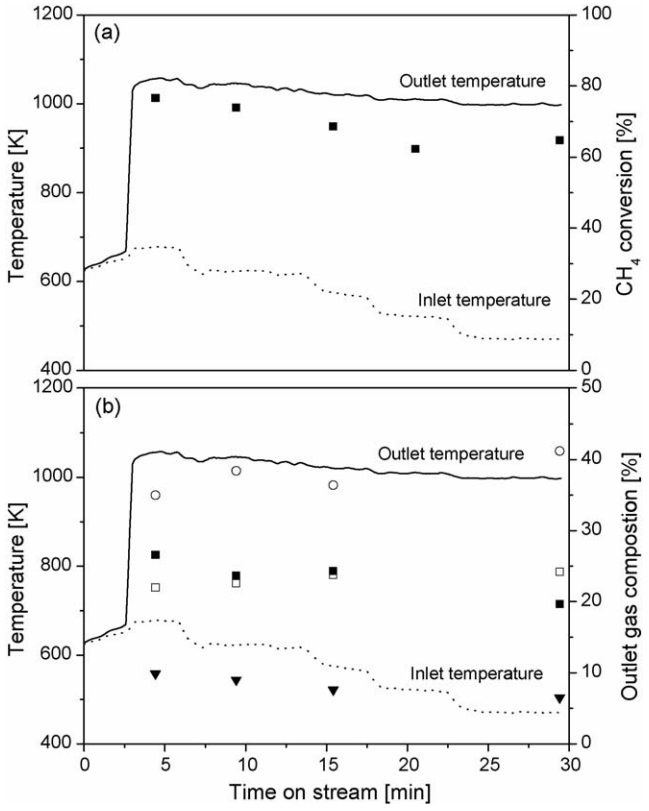

Fig. 3. Catalytic performance of 1% Rh/Ce-ZrO_2 at $\lambda = 0.25$: (a) methane conversion (■) and (b) outlet gas composition of H_2 (■), CO (▼), CO_2 (□) and H_2O (○).

higher temperatures when Ce is added and no transition occurs in the temperature range tested.

3.2. Activity tests

The activity of the catalysts was determined by slowly increasing the temperature of the inlet gas mixture (T_{in}) until light-off occurred, which was indicated by a rapid increase of the catalyst outlet temperature. Thereafter, the catalyst inlet temperature was decreased step-wise while measuring the methane conversion efficiency and outlet gas composition. The catalytic performance of 1% Rh/Ce-ZrO_2 at $\lambda = 0.25$ is presented in Fig. 3. For this catalyst, a light-off temperature of 654 K can be observed resulting in a methane conversion of 77%. The outlet gas mixture contained 27% H_2, 10% CO, 22% CO_2 and 35% H_2O. When the catalyst inlet temperature is decreased, a drop in methane conversion can be observed (64% at $T_{in} = 470$ K). Simultaneously, the outlet gas composition is altered resulting in lower amounts of H_2 and CO but increased concentrations of CO_2 and H_2O. The catalyst outlet temperature is only slightly decreased when lowering the inlet temperature, which results in a greater temperature difference over the catalyst length at lower inlet temperatures.

Similar trends to those of Fig. 3 in terms of activity, stability and syngas formation were observed for all catalysts. A summary of the catalyst performance at different reaction conditions is presented in Table 2. The support material had a significant effect on the light-off temperature whereas the Rh loading only had a minor influence. The temperature required for light-off increased in the following order: 1% Rh/Ce-ZrO_2 < 2% Rh/ZrO_2 < 1% Rh/ZrO_2 < 0.5% Rh/ZrO_2 < 1% Rh/α-Al_2O_3. Increasing the Rh loading from 0.5 to 2% decreased the light-off temperature by 28 K. Similar syngas production could be observed for the ZrO_2 and Al_2O_3 supported catalysts. However, the introduction of ceria resulted in improved syngas formation and higher H_2/CO ratios. Furthermore, a stable combustion behavior was observed for all Rh-based catalysts resulting in active catalysts at $T_{in} = 473$ K after ignition.

Results are presented in Fig. 4 for the 1% Rh/Ce-ZrO_2 catalyst, when the inlet methane concentration is reduced so as to achieve $\lambda = 0.40$. Light-off occurs at 688 K, which is higher than for $\lambda = 0.25$. Furthermore, increasing λ results in higher catalyst outlet temperatures, higher methane conversions, decreased hydrogen formation, higher H_2O concentrations and lower H_2/CO ratios. These observations imply a shift in reaction selectivity favoring total oxidation.

Table 2
Summary of catalytic performance during activity tests (conv = conversion of methane)

Catalyst			T_{in} = 623					T_{in} = 473				
	λ	$T_{light-off}$ [K]	T_{out} [K]	Conv [%]	H_2 [vol%]	CO [vol%]	H_2/CO	T_{out} [K]	Conv [%]	H_2 [vol%]	CO [vol%]	H_2/CO
0.5% Rh/ZrO_2	0.25	714	1129	71	14.4	6.6	2.2	1084	66	12.0	5.5	2.2
	0.40	784	1218	86	13.2	7.5	1.8	1144	76	12.7	6.5	2.0
1% Rh/ZrO_2	0.25	693	1050[a]	62[a]	18.9	8.1	2.3	1035	53	13.6	6.2	2.2
	0.40	723	1181[b]	90[b]	16.0[b]	9.0[b]	1.8[b]	–	–	–	–	–
2% Rh/ZrO_2	0.25	686	1017	69	18.8	7.7	2.4	981	56	18.0	6.3	2.9
	0.40	733	1195	91	15.9	9.8	1.6	1092	85	13.0	7.7	1.7
1% Rh/α-Al_2O_3	0.25	782	1025	60	18.4	7.9	2.3	990	48	13.8	6.1	2.3
	0.40	–	1170	87	13.9	8.6	1.6	1085	82	13.5	6.9	2.0
1% Rh/Ce-ZrO_2	0.25	654	1044	74	23.7	9.0	2.6	997	65	19.7	6.5	3.0
	0.40	688	1207	90	16.7	10.3	1.6	1112	87	15.8	8.5	1.9

[a] T_{in} = 633 K.
[b] T_{in} = 668 K.

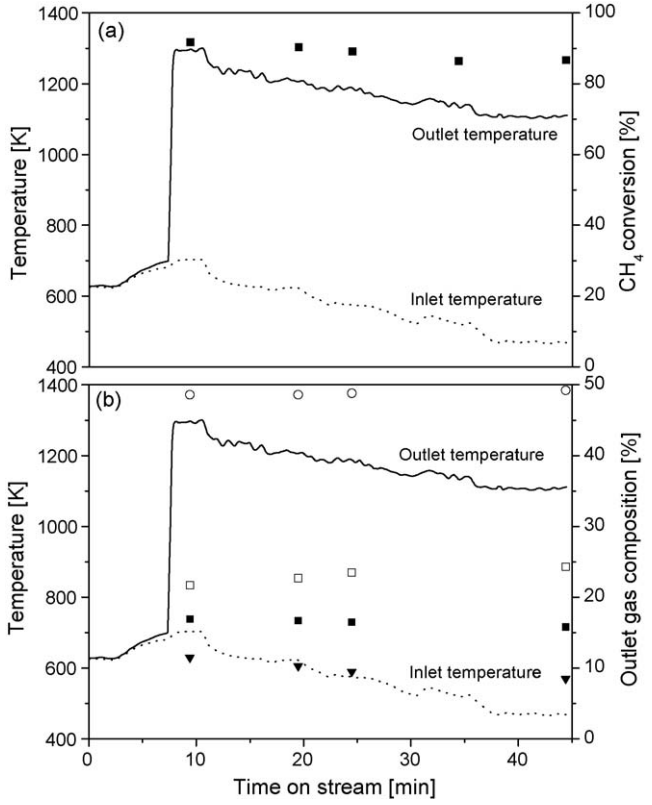

Fig. 4. Catalytic performance of 1% Rh/Ce-ZrO_2 at $\lambda = 0.40$: (a) methane conversion (■) and (b) outlet gas composition of H_2 (■), CO (▼), CO_2 (□) and H_2O (○).

4. Discussion

For the catalytic stage of the AZEP process described above it is important to achieve ignition temperatures in the range 723–823 K as this is the temperature of the inlet gas mixture and, therefore, preheaters could be avoided. The ignition temperature can be higher than that of conventional catalytic combustor systems since the recirculation of hot exhaust gas preheats the reactant mixture. Furthermore, the production of hydrogen is of importance for stabilizing the following homogeneous combustion stage. However, the very high selectivity for syngas production that is desired for other CPO processes, such as methanol and Fischer–Tropsch syntheses, is not as important in the present application.

The activation of the first C–H bond is generally considered to be the crucial step for oxidation of saturated hydrocarbons. For the catalytic partial oxidation of methane, this activation involves surface assisted dehydrogenation producing methyl radicals [12]. The oxidation state of the catalyst surface can have a strong effect on the hydrocarbon activation and, consequently, on the oxidation activity.

In a previous work by Buyevskaya et al. [13] the nature of the active surface sites of Rh catalysts for the CPO reaction was investigated. Here, neither a completely reduced nor a totally oxidized state of rhodium was found to be the most active sites for methane activation. Instead, partially oxidized species, Rh^+, or highly dispersed Rh^{3+} were proposed to act as active surface centers. Similar trends have been reported for methane oxidation over Pt catalysts [14]. In this study, a partially oxidized Pt surface is found to result in the optimum activity since the C–H bond activation is facilitated.

The XPS results presented in Fig. 2 show that Rh is present in a totally oxidized state in the fresh catalysts. However, the spectra obtained for used catalysts show that a partially reduced Rh surface is formed under reaction conditions. Although the TPR experiments were conducted under different reaction conditions than the activity tests, the results indicate that Rh_2O_3 is easily reduced ($T < 473$ K) for all catalysts such that a partially reduced phase may form prior to ignition.

The present activity tests show that inlet gas temperatures in the range of 654–782 K are required for light-off. The lowest light-off temperature (654 K) was obtained for the Rh/Ce-ZrO_2 catalyst. This is not surprising since a considerably higher Rh dispersion was measured for this catalyst. Metal dispersions of 44 and 21% were obtained for the 1% Rh/Ce-ZrO_2 and 1% Rh/ZrO_2 catalysts, respectively. A high dispersion of the active phase will provide more active sites for methane activation. The high dispersion is related to the presence of ceria in the support material and two influencing factors can be identified. First, the BET analyses show that the presence of Ce results in a higher surface area than for pure ZrO_2, which obviously would improve the dispersion of the active phase. This is related to the different ZrO_2 phases identified for the catalysts. The Raman microscopy analysis reveals that pure tetragonal zirconia is present in Rh/Ce-ZrO_2. For Rh/ZrO_2, the lower surface area monoclinic phase is also detected. The stabilization of tetragonal zirconia by incorporation of another metal cation, which acts as a sintering inhibitor, has been reported previously [15]. Rh/Ce-ZrO_2 is also expected to exhibit a more stable catalytic behavior since no phase transition of the support material occurs under reaction conditions, which is the case for zirconia. Secondly, ceria is known for its ability to interact strongly with noble metals under high temperature oxidizing conditions [16]. Therefore, if Ce atoms are homogeneously distributed in another metal oxide such as ZrO_2, the formation of M–O–Ce complexes during high temperature calcination would result in an improved dispersion. Furthermore, the high oxygen mobility of ceria may contribute to the high activity of Rh/Ce-ZrO_2 by enhancing the methane dissociation. The size of the rhodium particles could also have an influence on the methane activation. However, the particle size effect was not investigated in the present study.

The reaction conditions of AZEP are quite different than those of other CPO processes due to the high amounts of water and carbon dioxide of the former process. At lower temperatures, water is expected to adsorb on the catalyst. This could inhibit the active sites responsible for C–H bond activation. Therefore, desorption of water from the catalyst surface could be the rate determining step at lower temperatures where light-off occurs. Previous results on supported Rh catalysts for CPO have shown that the addition of water to the inlet gas mixture increased the light-off temperature considerably [6].

Different reaction mechanisms for the partial oxidation of methane to syngas have been proposed: (i) direct partial

oxidation forming CO and H_2 as primary products (1) and (ii) complete combustion forming CO_2 and H_2O (2), followed by methane reforming by steam (3) and CO_2 (4) yielding syngas.

$$CH_4 + \tfrac{1}{2}O_2 = CO + 2H_2, \quad \Delta H_{298} = -36\,\text{kJ/mol} \tag{1}$$

$$CH_4 + 2O_2 = CO_2 + 2H_2O, \quad \Delta H_{298} = -890\,\text{kJ/mol} \tag{2}$$

$$CH_4 + H_2O = CO + 3H_2, \quad \Delta H_{298} = 250\,\text{kJ/mol} \tag{3}$$

$$CH_4 + CO_2 = 2CO + 2H_2, \quad \Delta H_{298} = 247\,\text{kJ/mol} \tag{4}$$

Hickman and Schmidt reported that CO and H_2 are formed as primary products on Rh and Pt catalysts at high temperatures and short residence times [17,18]. Other studies also support the direct mechanism for syngas formation [19,20]. The indirect mechanism, where total oxidation of methane is followed by steam and CO_2 reforming, has been reported extensively [21–24]. Investigations by Weng et al. [25,26] show that the mechanism depends on the catalyst composition. The direct formation of CO and H_2 occurs on Rh/SiO_2 while total oxidation to CO_2 and H_2O is favored on Ru/SiO_2. Here, the difference in mechanism for partial oxidation of methane is related to the difference in the concentration of O^{2-} species over the catalyst. Clearly, the CPO reaction mechanism is not straightforward and depends on reaction conditions, catalyst composition, state of active metal and surface species present.

The main purpose of this study was not to investigate the mechanism for the CPO reaction. However, the results from the activity tests ($\lambda = 0.25$) indicate that an indirect route prevailed. The data presented in Fig. 3 and Table 2 show that the production of syngas is highest immediately after light-off when the catalyst temperature reaches a maximum. When the catalyst inlet temperature is decreased, followed by a slight decrease in exit temperature, the exit gas composition changes to lower amounts of syngas and slightly higher CO_2 and H_2O concentrations. The increased amount of CO_2 and H_2O at lower temperatures indicates that at lower conversions the complete oxidation is favored over the partial oxidation route. Furthermore, the indirect mechanism is supported by the fact that the temperature difference over the catalyst was always larger at lower conversions. This is related to the significantly higher exothermicity of the complete oxidation reaction.

H_2/CO ratios higher than 2 could be observed for all catalysts at $\lambda = 0.25$, which would be the expected value considering the stoichiometry of the partial oxidation reaction (1). Most likely, this is related to steam reforming and/or the water gas shift reaction (5). Ceria is known to promote the water gas shift and steam reforming reactions, which could explain why the highest concentrations of hydrogen are always observed for $Rh/Ce\text{-}ZrO_2$.

$$CO + H_2O = CO_2 + H_2 \tag{5}$$

Optimization of the active noble metal in the catalyst is of high importance due to the high costs of noble metals, Rh in particular. The results presented in Table 2 show that a slight decrease in light-off temperature is obtained when the Rh loading is increased. However, an increase from 0.5 to 2% resulted in a drop of the ignition temperature by only 28 K. The syngas production was mainly affected by increasing the loading from 0.5 to 1%. A study by Wang and Ruckenstein regarding partial oxidation of methane over supported Rh catalysts showed similar results [27]; therein, the activity and selectivity was found to increase for loadings between 0.01 and 0.5 wt% but remained constant at higher loadings.

5. Conclusions

The results presented here show that a hybrid combustor design consisting of a fuel-rich catalytic stage followed by H_2-stabilized homogeneous combustion is a promising combustion method for the AZEP concept. Supported rhodium catalysts are suitable for the light-off stage in the exhaust gas-diluted reaction mixtures that are present in the AZEP configuration.

The support material had a significant effect on the light-off temperature, which increased in the following order $Rh/Ce\text{-}ZrO_2 < Rh/ZrO_2 < Rh/\alpha\text{-}Al_2O_3$. The Rh loading, however, only had a minor influence, i.e. an increase from 0.5 to 2% decreased the light-off temperature by 28 K. The high activity of $Rh/Ce\text{-}ZrO_2$ is probably related to the high dispersion of Rh on $Ce\text{-}ZrO_2$ and the high oxygen mobility of this support compared to pure ZrO_2. The formation of hydrogen was also found to increase over the catalyst containing ceria in the support material. The activity tests indicated that the formation of syngas proceeded according to the indirect reaction mechanism consisting of complete combustion followed by reforming reactions. Upon ignition, all catalysts could sustain stable combustion even when the inlet temperature was reduced by as much as 200 K (i.e. $T_{in} = 473$ K) owing to the very strong ignition/extinction hysterisis.

Decreasing the inlet methane concentration, and thereby increasing λ from 0.25 to 0.40, resulted in higher light-off temperatures for all catalysts. Additionally, increasing λ generated higher catalyst outlet temperatures, higher conversions, decreased hydrogen formation, higher H_2O concentrations and lower H_2/CO ratios. These observations imply a shift in reaction selectivity towards total oxidation.

Acknowledgements

Financial support from the European Commission and the Swiss Government through the AZEP project, contract no. ENK5-CT-2001-00514, is gratefully acknowledged.

References

[1] T. Griffin, S.G. Sundkvist, K. Åsen, T. Bruun, Advanced Zero Emissions Gas Turbine Power Plant, ASME TURBO EXPO, Atlanta, GA, USA, June 16–19, 2003.
[2] R. Burch, F.J. Urbano, P.K. Loader, Appl. Catal., A 123 (1995) 173.
[3] J.C. van Giezen, F.R. van den Berg, J.L. Kleinen, A.J. van Dillen, J.W. Geus, Catal. Today 47 (1999) 287.
[4] P. Hurtado, S. Ordóñez, H. Sastre, F.V. Díez, Appl. Catal. B 47 (2004) 85.
[5] C. Appel, J. Mantzaras, R. Schaeren, R. Bombach, A. Inauen, N. Tylli, M. Wolf, T. Griffin, D. Winkler, R. Carroni, Proc. Combust. Inst. 30 (2005) 2509.

[6] S. Eriksson, M. Nilsson, M. Boutonnet, S. Järås, Catal. Today 100 (2005) 447.
[7] J.M. Gatica, R.T. Baker, P. Fornasiero, S. Bernal, G. Blanco, J. Kaspar, J. Phys. Chem. B 104 (2000) 4667.
[8] J.H. Scofield, J. Electron Spectrosc. Relat. Phenom. 8 (1976) 129.
[9] M.J. Guittet, J.P. Crocombette, M. Gautier-Soyer, Phys. Rev. B 63 (2001) 125117.
[10] NIST online database http://srdata.nist.gov/xps/.
[11] J.M. Moulder, in: J. Chastain (Ed.), Handbook of X-ray Photoelectron Spectroscopy, Perkin-Elmer Corp., 1992.
[12] R. Burch, M.J. Hayes, J. Mol. Catal. A 100 (1995) 13.
[13] O.V. Buyevskaya, K. Walter, D. Wolf, M. Baerns, Catal. Lett. 38 (1996) 81.
[14] R. Burch, P.K. Loader, F.J. Urbano, Catal. Today 27 (1996) 243.
[15] Z. Hy, J. Mater. Sci. 29 (1994) 4351.
[16] A. Trovarelli, Catal. Rev. Sci. Eng. 38 (1996) 439.
[17] D.A. Hickman, L.D. Schmidt, J. Catal. 138 (1992) 267.
[18] D.A. Hickman, L.D. Schmidt, ACS Symp. Ser. 523 (1993) 416.
[19] E.P.J. Mallens, J.H.B.J. Hoebink, G.B. Marin, J. Catal. 167 (1997) 43.
[20] K. Heitnes Hofstad, J.H.B.J. Hoebink, A. Holmen, G.B. Marin, Catal. Today 40 (1998) 157.
[21] W.J.M. Vermeieren, E. Blomsma, P.A. Jacobs, Catal. Today 13 (1992) 427.
[22] O.V. Buyevskaya, D. Wolf, M. Baerns, Catal. Lett. 29 (1994) 249.
[23] F. van Looij, E.R. Stobbe, J.W. Geus, Catal. Lett. 50 (1998) 59.
[24] T. Bruno, A. Beretta, G. Groppi, M. Roderi, P. Forzatti, Catal. Today 99 (2005) 89.
[25] W.Z. Weng, M.S. Chen, Q.G. Yan, T.H. Wu, Z.S. Chao, Y.Y. Liao, H.L. Wan, Catal. Today 63 (2000) 317.
[26] W.Z. Weng, Q.G. Yan, C.R. Luo, Y.Y. Liao, H.L. Wan, Catal. Lett. 74 (2001) 37.
[27] H.Y. Wang, E. Ruckenstein, Catal. Lett. 59 (1999) 121.